Three-dimensional geologic model of southeastern Tertiary coastal-plain sediments, Savannah River Site, South Carolina: An applied geostatistical approach for environmental applications

Guillaume A. Jean, Jeffrey M. Yarus, Gregory P. Flach, Margaret R. Millings, Mary K. Harris, Richard L. Chambers, and Frank H. Syms

ABSTRACT

A high-resolution geologic model of the General Separations Area supporting groundwater cleanup at the Savannah River Site (SRS) was developed using geostatistical approaches adapted from the petroleum industry. Depositional facies in each formation were identified from core descriptions and modeled using sequential indicator simulation. Petrophysical properties in each facies were then modeled as distinct fields using sequential Gaussian simulation. A complete property distribution was assembled as a montage of the three-dimensional fields simulated independently in each facies. Petrophysical property realizations thus reflect the spatial distribution of and sharp boundaries between facies. Application of sequence-stratigraphic principles was difficult because of the small scale of the study site, unconsolidated nature of sediments, and proximity to the Fall Line. Nevertheless, multidimensional variogram mapping was effective at identifying the underlying spatial structures in the field data needed to reproduce major preserved features of the ancient coastline in model surfaces and facies and property fields. Preliminary assessment of permeability fields derived from the geologic model using connectivity and streamline and tracer simulation suggests that the methods were successful in identifying preferential pathways for contaminant migration from the SRS F-area seepage basins. However, further analysis using a numerical solute transport model with rigorous boundary conditions is needed for confirmation.

Copyright ©2004. The American Association of Petroleum Geologists/Division of Environmental Geosciences. All rights reserved.

DOI:10.1306/eg.06150404011

AUTHORS

GUILLAUME A. JEAN ~ *Ecole Nationale Supérieure de Géologie, rue du Doyen Marcel Roubault, 54501 Vandœuvre-les-Nancy, France*

Guillaume Jean received his Diplome d'Ingenieur from the Ecole Nationale Superieure de Geologie (Nancy, France) in 2003. He is currently finishing an M.S. degree in petroleum engineering at Imperial College (London, United Kingdom). He will soon be working as a reservoir engineer in the petroleum industry.

JEFFREY M. YARUS ~ *Quantitative Geosciences LLP, 2900 Wilcrest, Suite 370, Houston, Texas 77042*

Jeffrey Yarus obtained his Ph.D. at the University of South Carolina in 1977 in geology, specializing in statistical applications. He has worked for a variety of petroleum and technology companies, including Marathon, GeoMath, Roxar, and Knowledge Reservoir. In 2001, Yarus started Quantitative Geosciences LLP with his partner Richard Chambers, with whom he has authored several papers and books.

GREGORY P. FLACH ~ *Savannah River National Laboratory, Savannah River Site, 773-42A, Aiken, South Carolina 29808; gregory.flach@srs.gov*

Greg Flach earned a Ph.D. in mechanical engineering from North Carolina State University in 1988. Since then, he has worked at the Savannah River National Laboratory on a variety of environmental and nuclear engineering topics, specializing in mathematical and numerical analysis and simulation.

MARGARET R. MILLINGS ~ *Savannah River National Laboratory, Savannah River Site, 773-42A, Aiken, South Carolina 29808*

Margaret Millings joined the Savannah River National Laboratory in February 2001 after receiving an M.S. degree in geology in 1997 from the University of Georgia and working several years in the environmental field. She has been involved as a geologist and geochemist in various projects pertaining to metals and dense nonaqueous-phase liquid contamination, geochemical modeling, and the geology of the Savannah River Site.

MARY K. HARRIS ~ *Savannah River National Laboratory, Savannah River Site, 773-42A, Aiken, South Carolina 29808*

Mary Harris is the geosciences manager for the Environmental Sciences and Technology Department at the Savannah River National Laboratory. She received her M.S. degree in geology from the University of Idaho and her Ph.D. in geological sciences from the University of South Carolina. One of her fundamental beliefs is that understanding subsurface geology provides the base for successful remedial technology deployments.

RICHARD L. CHAMBERS ~ *Quantitative Geosciences LLP, 2900 Wilcrest, Suite 370, Houston, Texas 77042*

Richard Chambers earned his Ph.D. in geology from Michigan State University. In 2001, he cofounded Quantitative Geosciences LLP with offices in Broken Arrow, Houston, and London. He is the current chairman of the AAPG Reservoir Development Committee.

FRANK H. SYMS ~ *Bechtel Savannah River Inc., Savannah River Site, Aiken, South Carolina, 29808*

Frank Syms is as engineering geologist for Bechtel, specializing in subsurface exploration in coastal-plain environments. He has B.S. and M.S. degrees and a Ph.D. from the University of South Carolina. Research interests include geologic interpretation of cone penetration data and sequence stratigraphy reconstruction in the Carolina coastal plain.

ACKNOWLEDGEMENTS

We wish to thank Earth Decision Sciences, Geovariances, and StreamSim for allowing us to use their respective state-of-the-art software. In addition, we wish to thank Quantitative Geosciences for their guidance and support on geostatistics. Finally, we are sincerely grateful to Westinghouse Savannah River Company and the U.S. Department of Energy for making this work possible and for the permission to publish our findings.

INTRODUCTION

Geostatistics provides numerous spatial analytical tools to interpolate or simulate variables at unsampled locations. These methodologies developed over the past 40 yr (Krige, 1951, 1966; Matheron, 1963, 1970, 1978; Isaaks and Srivastava, 1989), represent a vast improvement over traditional interpolation techniques that are limited in their ability to capture spatial continuity (Hohn, 1988; Yarus and Chambers, 1994). Geostatistical approaches have become routine practice in petroleum reservoir flow simulation but are still relatively uncommon in groundwater flow and contaminant transport simulations supporting environmental cleanup. From a business perspective, a contributing factor has been the relatively high cost of geostatistical software and expert analysts required to effectively apply geostatistics. The budget associated with a typical oil field can support such cost, whereas the average environmental cleanup site has a much smaller budget. Nevertheless, use of geostatistics in environmental remediation projects is increasing as the benefits of geostatistical modeling become more apparent and appropriate software less expensive.

In the present study, we adapt geostatistical technologies applied to the petroleum industry to environmental remediation needs in the General Separations Area (GSA) at the Savannah River Site (SRS). The GSA contains more than 35 active and closed groundwater contamination sites. Thus, the significance of the GSA justifies comprehensive reanalysis of the area from a geostatistical perspective. The study focuses on developing a realistic, fine-scale, three-dimensional, geologic model as a prerequisite to future groundwater flow and contaminant transport analyses.

In environmental applications, geostatistical kriging and conditional simulation are commonly performed directly on petrophysical properties with only cursory attention paid to the depositional facies associated with such properties. Such an approach ignores most of the geological content of the data because the model is based only on physical rock properties. For example, hydraulic conductivity estimates from well tests or sediment samples in an aquifer are commonly directly interpolated onto a numerical grid to create the conductivity field for a groundwater model. This approach largely ignores the spatial relationships among depositional facies in a heterogeneous aquifer that can be critical to understanding groundwater flow paths (e.g., a barrier island sand has a different spatial distribution when compared to a fluvial sand). Preferential pathways driving contaminant migration may be associated with a particular facies and defined by abrupt changes in permeability associated with facies boundaries. Therefore, capturing the structure reflected by the facies distribution is important in petrophysical property modeling. Furthermore, research has shown that permeability data from different facies comprise distinct statistical populations (Yarus et al., 2002). Thus, mixing petrophysical property data from different facies should be avoided in geostatistical modeling.

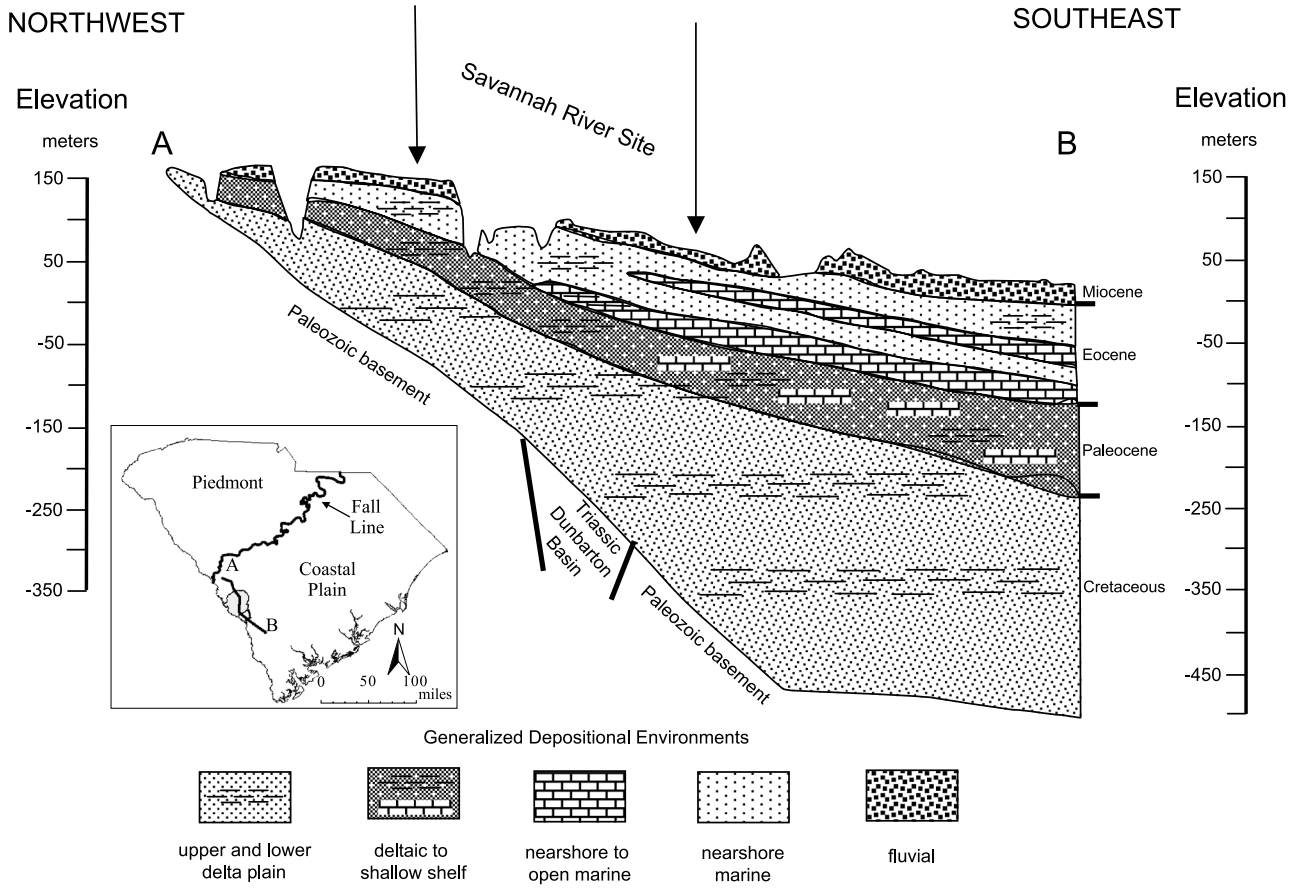

Figure 1. Generalized regional geologic cross section and physiographic location of the study area.

A key feature of the geostatistical approach employed in the present study is to first identify and spatially model the various depositional facies present in each aquifer zone. Petrophysical properties, such as mud content and permeability, are then modeled as distinct populations in each facies. The complete property field is assembled as a montage of the three-dimensional fields simulated independently in each facies, which occupies only a fraction of the total volume.

A challenge of the study was overcoming differences in the scale and types of characterization data available from an oil field vs. an environmental remediation site. Reservoir characterization and flow simulation are typically conducted at the basin scale: distances of 100 km^2 (39 mi) laterally, and depths to 3000 m (9800 ft). The extent of the General Separations Area is much smaller at 15 km^2 (6 mi^2) laterally and a depth of interest of less than 60 m (200 ft), uncompacted, below land surface. The difference in scale can make incorporating sequence-stratigraphic principles into the geologic model difficult because stratigraphic features that are typically described are larger than or similar in size to the GSA itself. The unconsolidated nature of much of the sediments underlying the SRS also makes modeling difficult because local correlative sedimentary structures and soil surfaces are poorly preserved. In addition, the position of the site relative to the Fall Line, i.e., the updip portion of the coastal plain, creates further challenges in geologic interpretations because of the significant role erosion can play in preserving the geologic record.

STUDY AREA

The SRS is an 800-km^2 (310-mi^2) U.S. Department of Energy reservation in southwestern South Carolina (Figure 1). Five nuclear reactors were constructed in the 1950s to produce nuclear materials for national defense, primarily tritium, and plutonium-239. Supporting facilities included two chemical separations plants, a heavy-water extraction plant, a nuclear fuel and target fabrication facility, a tritium extraction facility, and

Figure 2. Location of the GSA study area and characterization data.

waste management facilities. Today, the SRS is primarily engaged in the processing of legacy nuclear wastes, environmental cleanup, nonproliferation activities, and tritium recycling. The study area encompasses the General Separations Area in the center of the SRS (Figure 2).

The SRS lies in the Upper Atlantic coastal plain, a southeast-dipping wedge of unconsolidated and semiconsolidated sediment that extends from its contact with the Piedmont Province at the Fall Line to the edge of the continental shelf. The sediment ranges from Late Cretaceous to Miocene in age and comprises layers of sand, muddy sand, and mud with minor amounts of calcareous sediment. A representative geologic cross section through the study area is shown in Figure 1. Groundwater contamination is located primarily in the unconfined Upper Three Runs aquifer extending to the top of the Warley Hill Formation.

GEOLOGY

Characterization data in the form of well logs and cone penetration testing (CPT) data (cf. Lunne et al., 1997) are available at approximately 115 locations in the GSA (Figure 2). Geologic interpretations used in this investigation are based on numerous studies of coastal-plain sediments in the region (Pooser, 1965; Siple, 1967; Colquhoun and Johnson, 1968; Huddlestun and Hetrick, 1979; Colquhoun et al., 1982, 1983; Nystrom and Willoughby, 1982; Huddlestun, 1988; Dennehy et al., 1989; Logan and Euler, 1989; Nystrom et al., 1989, 1991; Harris et al., 1990, 1993; Robertson, 1990; Fallaw and Price, 1992, 1995; Robertson and Thayer, 1992). Figure 3 summarizes the lithostratigraphic units and depositional environment interpretations for the sediments beneath the GSA. Additional description for each formation is provided below.

Black Mingo Group (Lang Syne [Ellenton] Formation)

The Lang Syne (Ellenton) Formation consists of dark gray and black lignitic clay with interbedded, poorly to moderately sorted, micaceous and lignitic muddy quartz sand, and pebbly sand. The clay is fissile with laminae of micaceous silt and fine sand (Fallaw and Price, 1995). The gray and black lignitic fissile clay is interpreted as lagoonal or bay deposits, whereas the micaceous, lignitic muddy quartz sand and pebbly sand in the vicinity of the GSA is interpreted to have been deposited in an upper delta-plain environment (Figure 3). For this study, no depositional facies modeling was performed on this lithologic unit; however, it is the bottom unconformable surface used in the model.

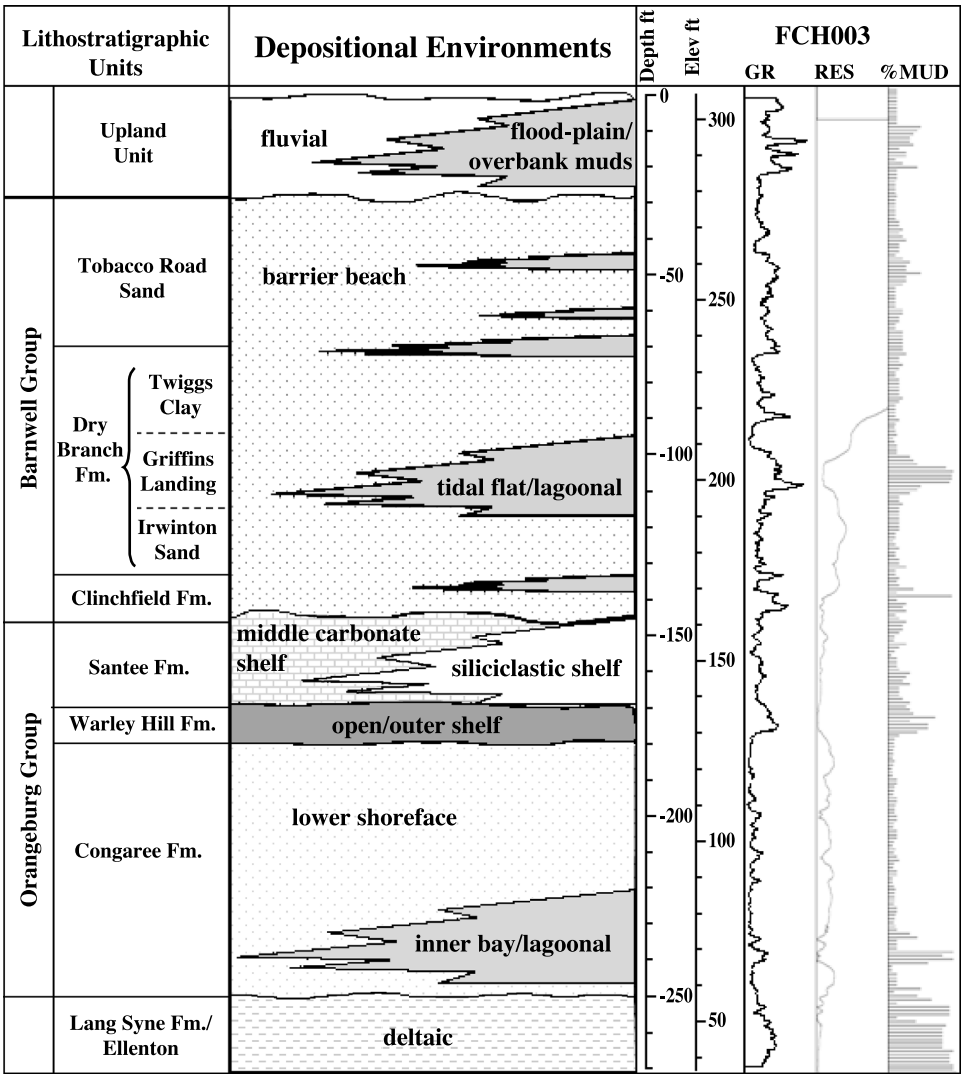

Figure 3. Lithostratigraphic units and associated depositional environments beneath the study area.

Orangeburg Group (Congaree, Warley Hill, and Santee Formations)

At the SRS, the Congaree Formation consists of yellow, orange, tan, gray, and greenish gray, iron-stained, moderately to poorly sorted, medium- to fine-grained sand, with discontinuous lenses of montmorillonite-rich clay (Colquhoun and Johnson, 1968). Layers rich in pebbles, clay clasts, calcareous sand, and glauconite are present but sporadic in their position in the formation. The base of the formation is unconformable. The Congaree and other deposits of lower middle Eocene age become increasingly calcareous between the SRS and the Atlantic Coast, where they are primarily limestone (Colquhoun et al., 1983; Harris et al., 1990, 1993). The updip portion of the Congaree in the study area represents lower shoreface and inner bay and lagoonal deposits.

The Warley Hill Formation unconformably overlies the Congaree Formation and consists of approximately 15 ft (5 m) of poorly to well-sorted quartz sand, commonly glauconitic, clay, sandy clay, and clayey sand (Fallaw and Price, 1995). Northwest of the study area, the Warley Hill is missing or very thin. The lithology of the Warley Hill Formation indicates deposition in a shallow to deep-water clastic shelf environment, generally deeper water than the underlying Congaree Formation (Pooser, 1965). Fallaw and Price (1995) note that the presence of glauconite and the dinoflagellate assemblage are indicative of shallow-marine conditions. The muddier sand in the Warley Hill indicates quieter water than that in which the Congaree was deposited (Fallaw and Price, 1995). For this study, the Warley Hill Formation was interpreted as the maximum flooding surface (MFS) in the study area.

The Santee Formation consists of moderately sorted, yellow, and tan sand, calcareous sand and clay, and terrigenous clay. The carbonate lithology of the Santee Formation includes tan to white calcilutite, calcarenite, shelly limestone, and calcareous sand and clay. Limestone is much more abundant in downdip areas, sporadic and podlike in the middle of the study area, and missing in updip areas northwest of the GSA. Within the study area, the Santee represents low- to high-energy, marine, middle-shelf depositional environments.

Barnwell Group (Clinchfield, Dry Branch, Tobacco Road Formations)

The Clinchfield Formation, the lowermost formation of the Barnwell Group, consists of medium-grained, well-sorted, poorly consolidated, and massively bedded quartz sand (Huddlestun and Hetrick, 1979). At the SRS, this unit has only been identified where carbonate strata of the Griffins Landing Member of the Dry Branch Formation and the Santee Formation are present, with sand of the Clinchfield between them. Within the GSA study area, this unit is interpreted to represent barrier beach-type deposits.

Huddlestun and Hetrick, 1979 divided the Dry Branch into three lithofacies: the Twiggs Clay, a marine, montmorillonite-rich clay; the Irwinton Sand, a distinctly bedded sand and clay; and the Griffins Landing Member, a massive calcareous and fossiliferous sand. The Griffins Landing contains the large oyster, *Crassostrea gigantissima*, and at updip (northwestern) locations, the clay matrix appears very similar to the Twiggs Clay and is probably correlative with this unit. The presence of *Crassostrea*-bearing beds indicates bay or lagoonal environments for the Griffins Landing Member. Sand of the Irwinton is interpreted to be inner neritic and barrier island deposits and the Twiggs Clay as lagoonal or possible bay deposits (Fallaw and Price, 1995).

The Tobacco Road Sand, the uppermost unit of the Barnwell Group, varies from fine-grained and well-sorted to poorly sorted sediment with pebbles. Variations in clay, chert, mica, carbonate, and heavy-mineral content exist locally (Huddlestun and Hetrick, 1979). Massive bedding and bioturbated strata characterize the formation (Logan and Euler, 1989). Abundant Ophiomorpha and clay laminae in the Tobacco Road Formation indicate deposition in a low-energy, transitional marine environment, such as a tidal flat (Fallaw and Price, 1995).

Upland Unit

The term upland unit has been widely used in the coastal plain of South Carolina for the poorly sorted, silty, clayey, and pebbly sand present at higher elevations in the study area. At the SRS, the upland unit has been called the Hawthorn Formation (Siple, 1967) and the Altamaha Formation (Huddlestun, 1988; Fallaw and Price, 1995). As the age of the unit is still controversial, this study used the informal name upland unit. The upland unit is considered by many to be a distinct unit separated from the underlying parts of the section by a significant unconformity (Nystrom and Willoughby, 1982; Nystrom et al., 1989). Within the study area, the upland unit is interpreted to represent fluvial and flood-plain deposits.

METHODS AND RESULTS

The workflow chosen for using geostatistical techniques in the current environmental project is comprised of the following major elements:

1. Horizons construction: define stratigraphic boundaries separating major geologic units using two-dimensional variograms and kriging
2. Stratigraphic grid construction: build three-dimensional grids occupying the space between horizons in a manner consistent with depositional environments
3. Depositional facies modeling: using depositional facies data from boreholes simulate the distribution of depositional facies over the three-dimensional stratigraphic grids for each formation
4. Petrophysical property modeling: using petrophysical property data defined from boreholes and CPT, simulate the three-dimensional distribution of the petrophysical property based on a chosen depositional facies distribution.

As mentioned earlier, step 3 is a key component of the present workflow and commonly omitted in petrophysical property modeling of aquifers. Depositional facies modeling ensures that the subsequent petrophysical property field will reflect sharp boundaries between facies where they exist and spatial continuity present in individual facies, which may define preferential pathways for contaminant transport. In describing each step below, emphasis is placed on those aspects that differ from typical workflows employed in the petroleum industry.

Surface Modeling

Structural modeling is a key to achieving geomodel quality and reliability in most oil reservoir studies. In addition to defining the large-scale geometry of the model, structural surfaces also impact the interwell distribution of petrophysical properties through the stratigraphic grid, which typically conforms to the former in some manner. Developing a sound structural model is difficult because geological surfaces are the result of complex deposition and erosion processes, and limited data (e.g., well picks) are available especially in environmental applications where seismic data are not obtained routinely. The different multidimensional geometrical features of a horizon, which can be observed in analogs with a greater extent, are related spatially. For instance, levee deposits are proximal to channel deposits, both having parallel geometries, but different petrophysical properties. Further, sequence-stratigraphic relationships are predictable and, thus, a preferred method for incorporating the commonly limited geologic information available into the surface models to the greatest extent.

Unfortunately, the relatively small scale of the GSA study area (15 km^2; 6 mi^2), the unconsolidated nature of the underlying sediments, and proximity to the Fall Line, make incorporating sequence-stratigraphic principles into the surface model difficult compared to studies of petroleum basins, as noted earlier. However, the shallow depth of the deposits and lack of compaction or tectonic deformation make the preservation of the original geomorphology and, thus, related facies geometries more likely.

Stratigraphic horizons were identified at approximately 115 locations in the GSA based on available characterization data (Figure 2). Characterization data used to distinguish these boundaries included geophysical logs (gamma ray and resistivity), CPT logs, and foot-by-foot core descriptions. These horizons mark significant changes in depositional environments with regard to relative sea level. The particular boundaries identified included the tops of the Tobacco Road, Santee, Warley Hill, Congaree, and the Lang Syne (Ellenton) formations. Among these, the top of the Warley Hill Formation, interpreted as the maximum flooding surface, was most easily identified.

Two-dimensional variogram maps were calculated to characterize the spatial correlation of each of six horizons. A two-dimensional variogram map is an experimental covariance graph calculated from the distance between pairs of points at varying separation intervals where there are measured surface altitude and depth data. The presence or absence of spatial correlation structures is affected by data sampling (e.g., sparseness), in addition to geologic features that are actually present. By analyzing a smoothed experimental variogram map of each horizon and interpreting the geologic features compatible with each depositional environment depicted in Figure 3, one or more geologic structures characterized by their orientation and maximum distance of correlation were identified. For example, the likely orientation and size of the paleocoast, inlets, and sand bars were used to set the direction and correlation length of multiple structures in model variograms. The experimental variogram map for the top of the Barnwell group is shown in Figure 4. Maximum continuity is seen along a southwest-northeast orientation reflecting the paleocoast. Shorter range continuity is also observed in northwest-southeast and is interpreted to possibly reflect channels and barrier islands related to a tidal delta system.

The variogram models were then used to interpolate the different surfaces using kriging-based methods (Matheron, 1978; Isaaks and Srivastava, 1989), which reproduces the spatial correlation defined by the variogram model and honors the input data. Five horizons were interpolated by ordinary kriging: the top of the Barnwell Group; the top of the Twiggs Clay Member of the Barnwell Group; the top of the Santee; the top of the Warley Hill (maximum flooding surface); and top of the Congaree. The deepest surface, the top of the Ellenton, was interpolated by a collocated cokriging method, because of very few well penetrations. This algorithm integrates a secondary data set as a soft trend (implying a structural correlation) into the interpolation process, in this case the kriged top of the Congaree surface.

An interesting surface is the top of the Barnwell Group, which exhibits geologic features similar to those seen in a modern-day analog, the present South Carolina coast. In Figure 5, the surface is compared to an aerial photo of Price Inlet, South Carolina (photo by Walter J. Sexton), which shows a tidal inlet, sand barriers, and a lagoon. The top of the Barnwell Group appears to show similar features of an appropriate scale that have been preserved in the geologic record and is consistent with the depositional environment interpretations.

Stratigraphic Grid

A stratigraphic grid representing the workspace volume was generated by discretizing the subsurface volume between the Ellenton (Lang Syne) horizon and

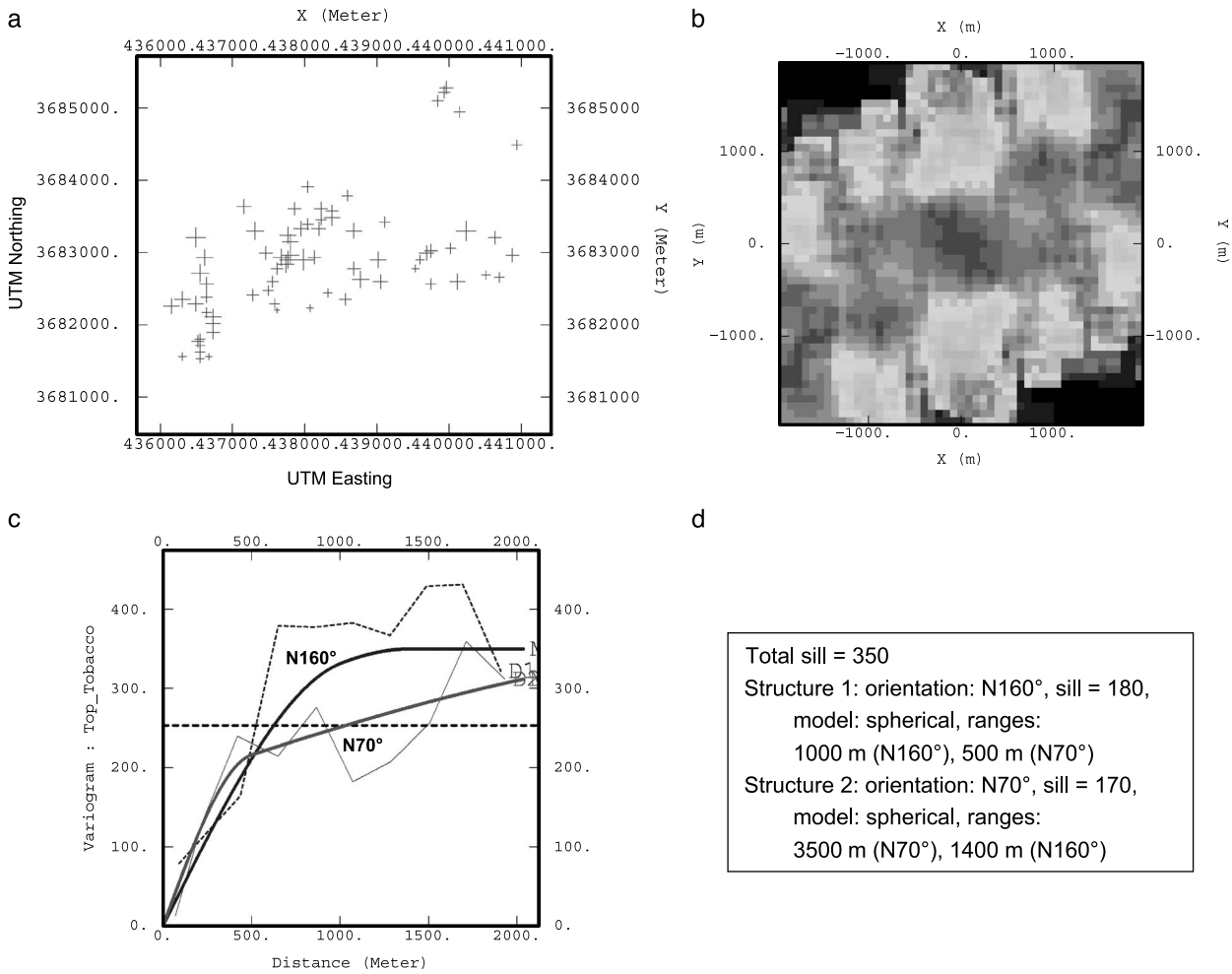

Figure 4. (a) Data location map, (b) variogram map, (c) variogram, and (d) variogram parameters of the top of the Barnwell Group.

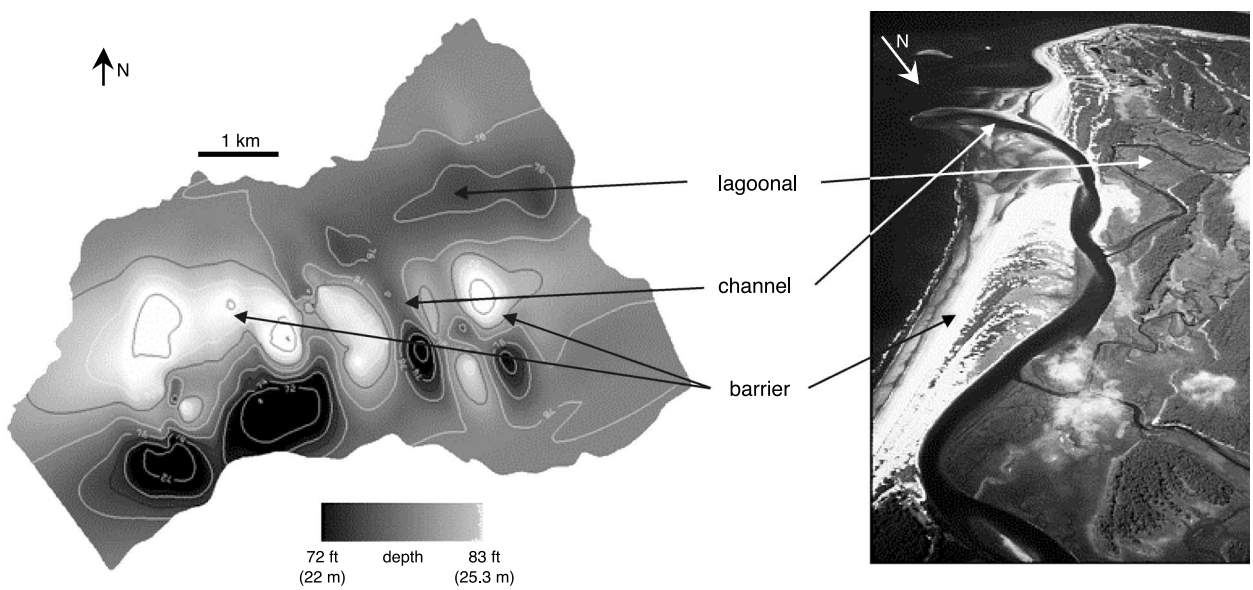

Figure 5. Top view of the top of Barnwell Group and an aerial photo of the coastline surrounding Price Inlet, South Carolina, a modern analog for the Barnwell Group (photo courtesy of Walter J. Sexton).

the ground surface, based on the structural model. In addition to defining the resolution of the model, the stratigraphic grid also constrains how petrophysical properties are spatially correlated across the interwell space. The horizontal grid orientation was set so that one axis is parallel to the paleocoastline. For this project, the maximum flooding surface represents a conformable surface. All other surfaces were unconformable. Therefore, the stratigraphic grid layering was defined to be parallel to the maximum flooding surface for the whole model. This implies erosional truncation boundaries with the other horizons, especially with the ground surface. This vertical gridding assumed that each concerned formation was deposited conformably to the maximum flooding surface. The grid cell size used was $\Delta x = \Delta y = 50$ m (160 ft) and $\Delta z = 0.61$ m (2 ft).

Depositional Facies Modeling

Following the conceptual model of depositional environments depicted in Figure 3, depositional facies logs were derived from core data and recorded using indicator values. To characterize the spatial correlation of the different facies, a variogram analysis using three-dimensional maps was performed for each facies in each stratigraphic unit (except the Warley Hill, which contains only one facies). Because the variograms are the same when there are only two facies present (Galli et al., 1994), of the symmetry of the variogram, only one analysis was done for units containing two facies. The analysis integrated well-log data and geologic interpolation guided in part by modern-day analogs, e.g., the current depositional environment along the South Carolina coast. The variogram ranges obtained in this manner, corresponding to the typical correlation distance of a facies object, were typically between 500 and 1000 m (1600 and 3300 ft). These correlation distances are typical of such depositional systems. The correlation orientations commonly coincided with the orientation of the actual coastline or the perpendicular direction, as expected. Multistructure variogram models were used to capture the spatial correlation in detail. Figure 6 shows the variogram map and the variogram model (containing two structures) of the Barnwell Group depositional facies. The first structure, oriented N45°, corresponds to the coastline correlation and the second one to channels and tidal delta system-related geological objects like sand barriers.

For facies and petrophysics modeling, it is commonly advisable to use a method that fully reproduces heterogeneity or variance in the model prediction. Kriging-based simulation methods are available for this purpose. These simulation methods attempt to reproduce the variability around the estimated value provided by kriging. Depositional facies were distributed in the interwell space using sequential indicator simulation separately in each formation. One sequential indicator simulation distributes all the facies in a selected formation, while honoring the variogram model and the well data. Two hundred simulations of depositional facies were run for each formation, and each simulation is equiprobable. Figure 7 shows the entire model with a particular facies simulation stacking arrangement described later. The facies distribution heterogeneities can be observed vertically and horizontally in terms of facies-facies boundaries and formation-formation boundaries.

One or more depositional facies distributions must be selected as a template for petrophysical property simulation. In this project, two approaches were considered. The first was to choose the most commonly occurring depositional facies at each grid location. The second strategy was to order or rank the depositional facies realizations according to a certain criterion presented later in the paper and choose the three realizations corresponding to 10, 50, and 90% cumulative probability levels (P10, P50, and P90).

The first approach has the advantage of not requiring a ranking criterion. However, the distribution defined by the most common facies at each location does not guarantee that the spatial correlation and global proportions of facies deduced from the data through spatial modeling will be honored. Specifically, the most common facies is biased toward the major facies in terms of global proportions in the formation, and the facies distribution does not have the finer scale heterogeneity of a simulation. The P10, P50, and P90 simulations in the second approach guarantee the proper spatial continuity and facies proportions on average but are dependent on a nonunique ranking process. The ranking algorithm chosen in this study is presented later.

Petrophysical Property Modeling

The petrophysical properties considered in the present study were the percentage of mud from core data and friction ratio (cf. Lunne et al., 1997) from CPT. Both properties provide an indirect indication of sediment permeability. For each facies in a formation, a variogram model was defined for percent mud using experimental variogram maps and geological interpretation.

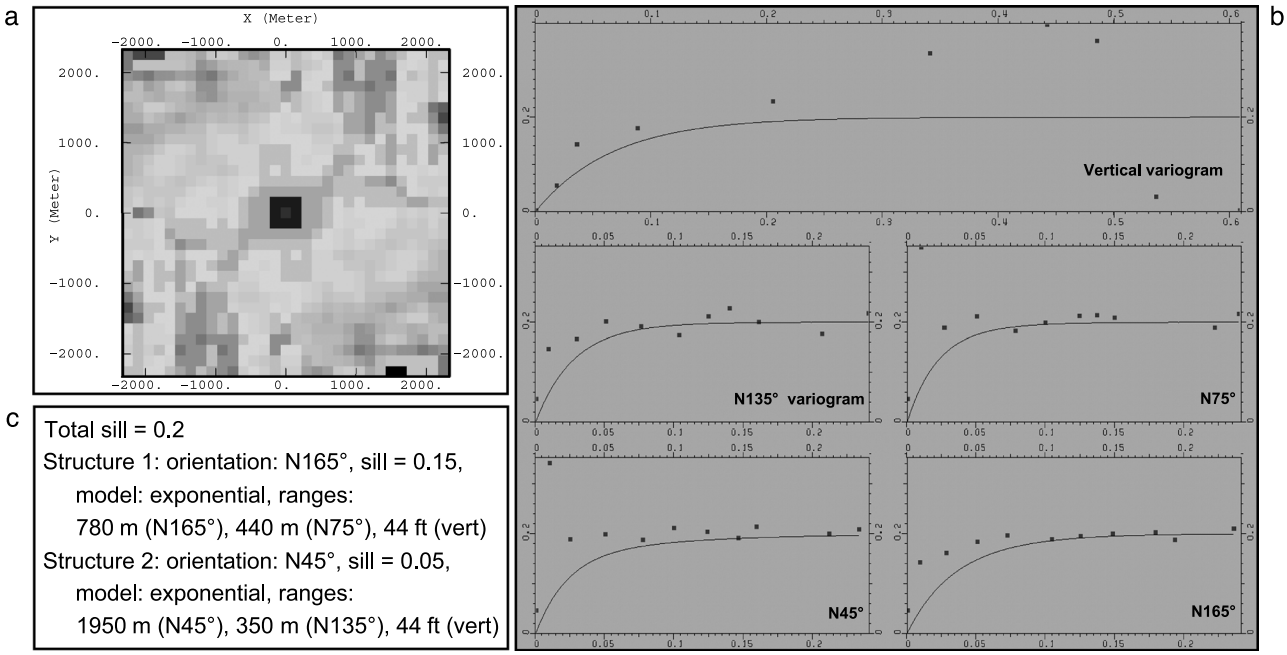

Figure 6. (a) Variogram map, (b) variogram, and (c) variogram model parameter of the depositional facies of the Barnwell Group.

For example, in the upland formation, two depositional facies (fluvial and flood-plain-overbank muds) are present; one variogram for percent mud was calculated in the fluvial facies using only the data occurring in this particular facies, and another variogram for flood-plain-overbank muds. The spatial distribution of percent mud is peculiar to each depositional facies because it is controlled by different processes of accumulation and erosion. Figure 8 represents the variogram map and the variogram of percent mud in one facies (middle shelf low energy) of the Santee Formation. A nugget effect was introduced because of the limited data reliability. The variogram map shows a correlation along a direction perpendicular to the coastline as found for some particular facies.

Similar to the facies modeling, kriging-based simulation was chosen to reproduce the heterogeneity of percent mud based on the variogram analysis. Friction ratio data were used as soft data through collocated cokriging where warranted. In general, however, CPT data were found to be poorly correlated with percent mud and thus made only a minor contribution to the collocated cokriging system. The lack of a good correlation was counterintuitive and may be an artifact because of postprocessing upscaling of the CPT data. Further analysis of this data is warranted.

Two hundred sequential Gaussian simulations were run separately in each depositional facies for each formation. A cell-by-cell postprocessing calculated the maximum, the minimum, the mean, and the standard deviation from each set of 200 simulations. The different petrophysical simulations corresponding to the different facies present were combined to form one global simulation over the sequence. After this combination

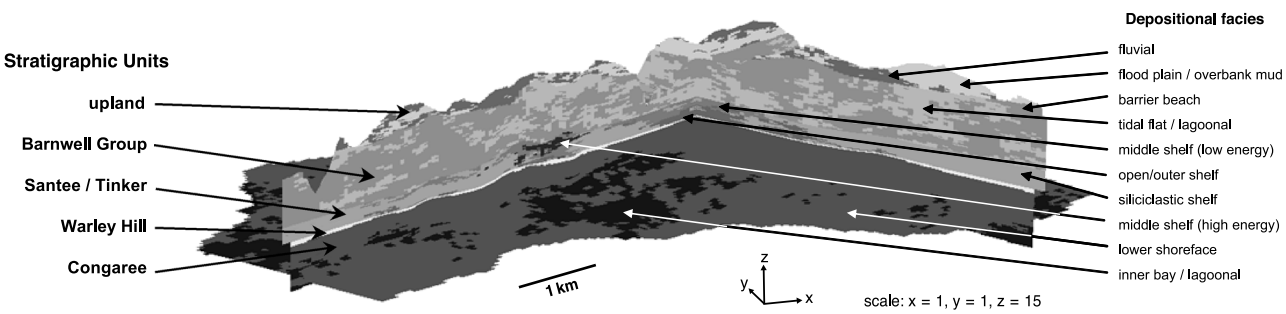

Figure 7. Vertical and areal cross sections of the whole model showing P50 simulations stacking arrangement of depositional facies.

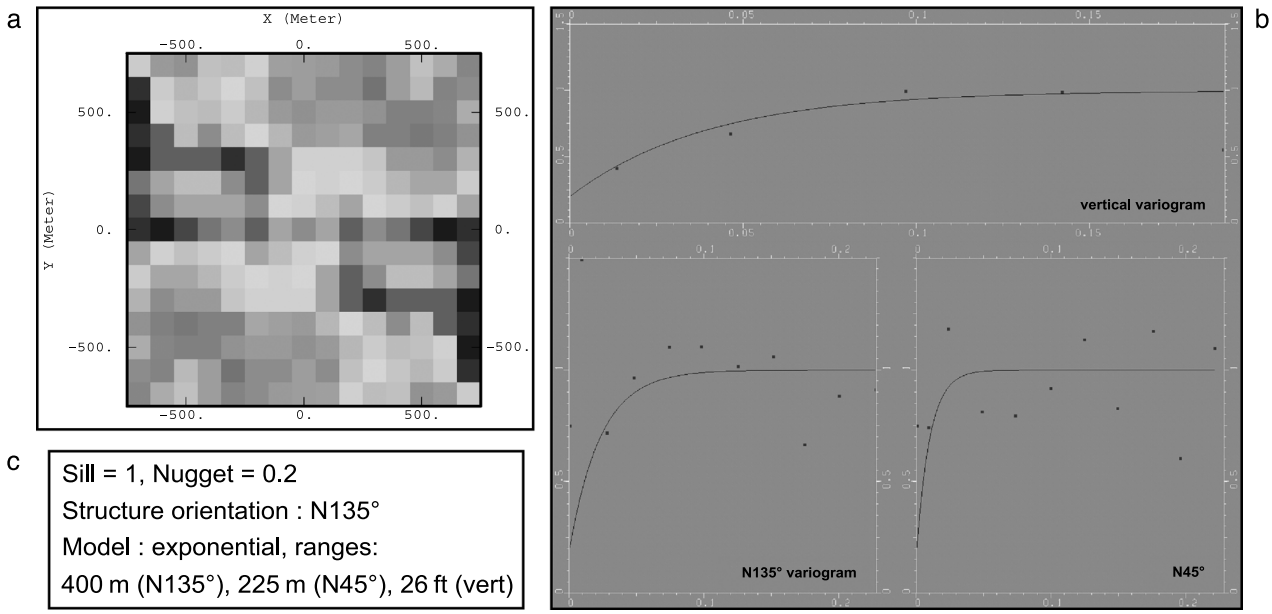

Figure 8. (a) Variogram map, (b) variogram, and (c) variogram parameters of percent mud calculated in a facies (middle shelf low energy) of the Santee Formation.

process, the 200 global petrophysical simulations were ranked separately for each sequence. The simulation ranking was achieved by defining a criterion that is described later. For each stratigraphic sequence, among the 200 equiprobable simulations of mud percentage, three of them (P10, P50, and P90) were chosen for further study. Figure 9 shows a particular stacking arrangement, discussed later, of different percent mud simulations for the entire model. Percent mud heterogeneities can be appreciated by different ways: facies related and stratigraphic formation related.

APPLICATION TO ENVIRONMENTAL REMEDIATION

To assess the potential merits of geostatistical modeling for environmental cleanup applications, we focused on investigating the impact of geology on contaminant migration from the former F-area seepage basins to Fourmile Branch (Figure 2). The unlined earthen basins in F-area were designed to receive low-level radioactive wastewater from the 200-H separations facilities and to filter out most radionuclides through sorption onto shallow native sediments. The basins operated in this mode from 1955 to 1988, after which they were closed and capped under the Resource Conservation and Recovery Act. The site has been extensively monitored and characterized through monitoring wells, CPT, and seepline sampling, resulting in a well-defined tritium plume. Figure 10 illustrates the monitoring data and a simulated tritium plume based on a conventional groundwater flow model with a relatively homogenous conductivity field (Flach, 2002). The conventional model predicts a broad plume of relatively uniform concentration in the center portion. In contrast, the monitoring data indicate a more narrow, preferential path located east of the center with respect to the simulated plume.

A complete life cycle analysis of the waste site would include formal groundwater flow and contaminant transport simulation and remediation design optimization and assessment, both of which were beyond the scope of the present investigation. Nevertheless, a preliminary analysis of permeability distribution was performed as an initial step toward achieving the latter goals. Specifically, high-permeability connectivity analysis and rudimentary groundwater streamline and plume tracer simulations were performed near F-area seepage basins. All three analyses can provide insights into contaminant plume migration and optimal remediation. As a prerequisite to these analyses, ranking criteria for the facies and petrophysical property simulations discussed previously were first developed.

Simulation Ranking and Stacking Strategy

In developing the ranking strategy, permeability is assumed to correlate strongly with the amount of mud (clay and silt) present: the more mud present in a zone, the lower the permeability. For each formation

Figure 9. Percent mud field corresponding to the second stacking arrangement (P10 in upland, P90 in Barnwell Group, etc.).

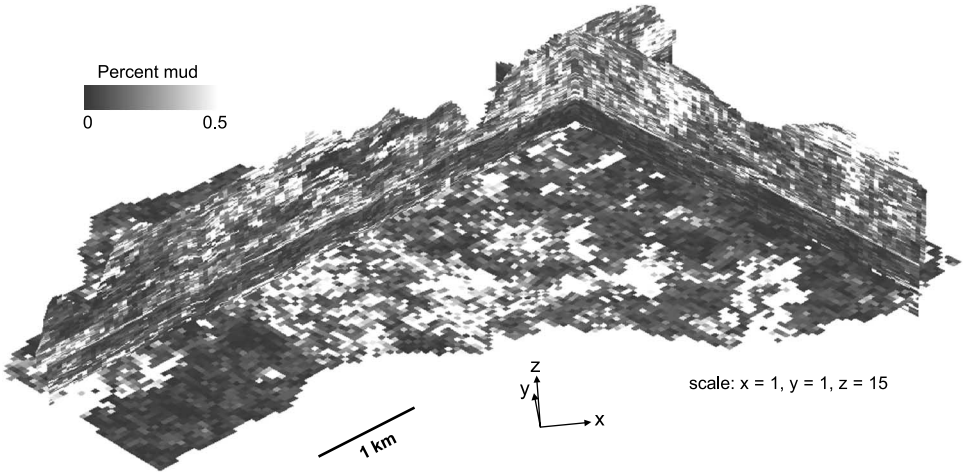

Figure 10. Tritium monitoring data and simulated plume based on a conventional groundwater flow model. See Figure 2 for location of the map.

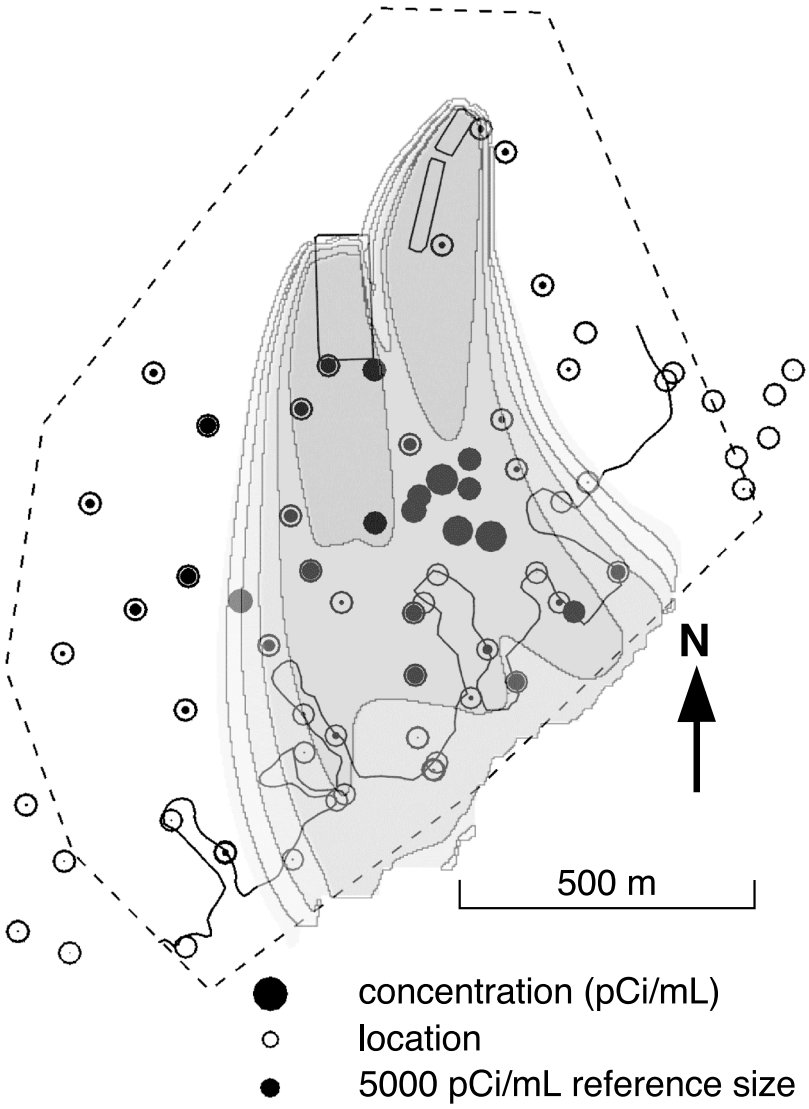

zone, the depositional facies interpreted to contain the most mud on average was identified. The facies simulations were then ranked by proportion of that facies present in a realization, with the proportion being calculated only over the F-area basins subregion. Similarly, the petrophysical simulations were ranked using the average value of percent mud calculated over the F-area subregion for each formation zone. This average value of percent mud was calculated using percent mud values from all facies present in the area. Realizations exhibiting median mud content were constructed for each formation by combining the P50 depositional facies simulations with the P50 percent mud simulations based on the former. Similarly, realizations exhibiting relatively low (high) permeability were generated by combining the P50 facies simulations (Figure 7) with the P10 (P90) property simulations also based on the former to avoid extremum permeability cases.

Three stacking arrangements were considered for the entire assemblage of five horizons:

- P50 in each formation for facies and percent mud,
- P50 for facies everywhere and P10 in the upland, P90 in the Barnwell, P10 in the Santee, etc. for percent mud (Figure 9),
- P50 for facies everywhere and P90 in the upland, P10 in the Barnwell, P90 in the Santee, etc. for percent mud.

The first arrangement produces the median result from a global perspective. The second scheme corresponds to higher mud content in aquifer zones and lower mud in confining zones, which would tend to produce deeper and slower groundwater flow. The third scheme produces the opposite effect of more shallow and faster groundwater flow from the waste site to surface discharge.

Connectivity Analysis

In preparation for connectivity analysis, permeability fields corresponding to the three stacking arrangements presented above were generated using the following correlation based on field and laboratory data:

$$k = 0.366D \times \begin{cases} \exp[(-12 \cdot \text{mud} + 2.4)\ln 10] & \text{mud} \leq 0.45 \\ \exp[(-3.273 \cdot \text{mud} - 1.527)\ln 10] & \text{mud} > 0.45 \end{cases} \quad (1)$$

Second, the different permeability models built for the entire GSA were downscaled in the F-area subregion from a 50 × 50 × 0.61 m (160 × 160 × 2 ft) resolution to 15 × 15 × 0.30 m (49 × 49 × 1 ft) using a geostatistical approach. Downscaling produced a model resolution more appropriate for the smaller scale F-area subregion.

Figure 11 shows cells with permeability in the range of 25–100 d in the third ranking and stacking scenario discussed above. Groups of cells are ranked and shaded by the extent of facies connectivity. Figure 11 also shows the monitoring data from Figure 10. The region immediately east-southeast of the basins lacks a preferential pathway for groundwater flow in the connectivity simulation, as evidenced by the absence of any significantly connected bodies of high-permeability sediment. Instead, the simulation indicates a preferential flow path starting immediately south of the largest basin and curving to the southeast near wetland discharge areas, which is consistent with the field data.

Streamline and Tracer Plume Simulation

The connectivity analysis considers only the potential impact of high-permeability pathways on contaminant migration. Hydraulic gradients caused by groundwater recharge and discharge areas also affect plume migration. A preliminary analysis of the both effects was conducted through crude streamline and tracer plume simulations, using software developed for oil field application.

One concern with streamline simulation involved setting up suitable hydrologic boundary conditions for the model. Contrary to the petroleum industry where flow is mainly initiated and sustained by well fluid injection, natural shallow groundwater flow is driven by rainfall, gravity, and discharge to low-lying wetlands and streams. In this case study, because of oil industry software limitations in hydrogeological modeling, rainfall was modeled by very shallow-water injection horizontal wells located along the ground surface. The injection rate was set to estimated recharge flux (0.30 m/yr; 1 ft/yr) times surface area. The stream that bounds F-area was represented by a producer well with a flow rate set to the estimated baseflow along the reach. Leakage from the bottom surface of the model to an underlying aquifer (0.075 m/yr [0.25 ft/yr] estimated) was reproduced by additional horizontal producer wells spread across that surface. The lateral bounds of the model were set to coincide with natural

Figure 11. Grid cells with 25–100-d permeability shaded by degree of connectivity. See Figure 2 for location of the map.

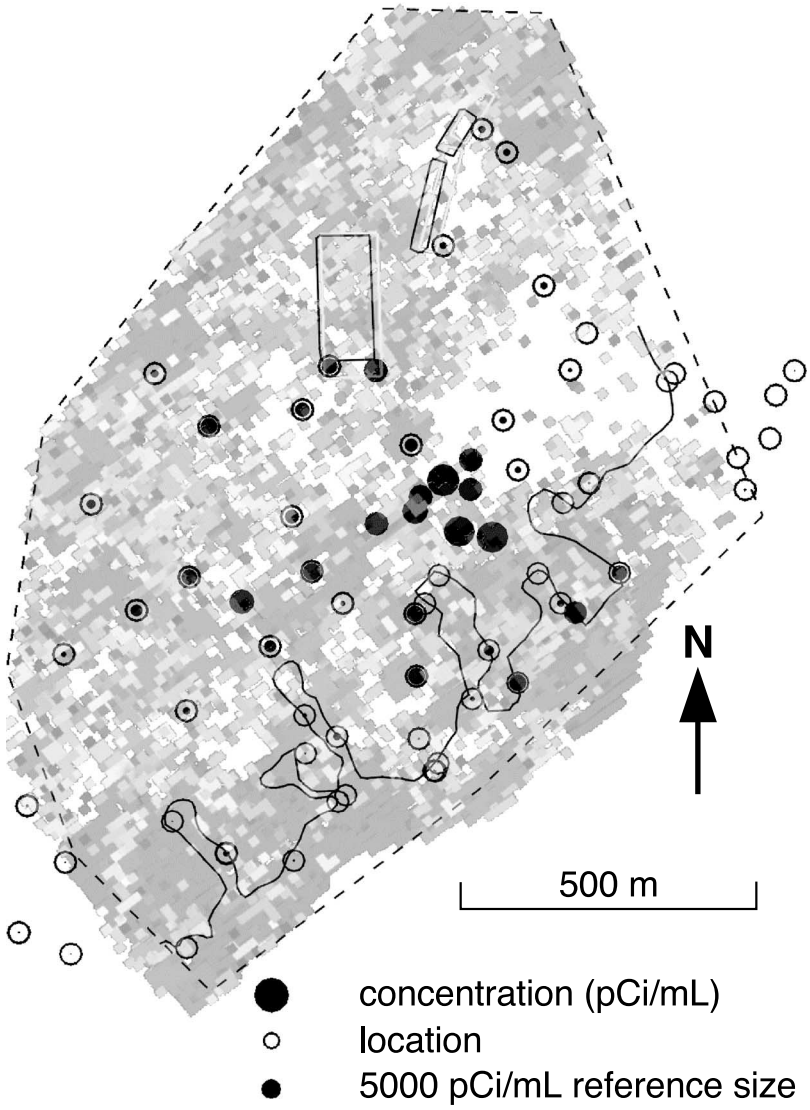

no-flow boundaries. The contaminant source was modeled by two very shallow vertical wells injecting a tracer, oil in the software, with fluid properties set to those of water. The permeability field was used as is in simulations and not calibrated to any monitoring data.

Figure 12 compares simulated contaminant migration from the F-area seepage basins to Fourmile Branch for the present high-resolution geologic model to plume data. The tracer simulations based on the present geostatistical model appear to align well with the preferential pathway indicated by the monitoring data. Although the present results are promising, additional effort is needed to transform the high-resolution permeability fields into a calibrated groundwater flow and solute transport model for a rigorous comparison to field data.

CONCLUSIONS

The main conclusions drawn from this work are as follows. Multidimensional variogram mapping was effective at identifying the underlying spatial structures in the field data needed to reproduce major preserved features of the ancient coastline in model surfaces, even with the challenges of applying sequence-stratigraphic principles in the area. Abrupt changes in physical properties associated with facies boundaries were reproduced in geostatistical simulations by modeling depositional facies and petrophysical properties in each facies in a two-step sequential process. Petrophysical property realizations reflect the distribution of facies inferred from data and preserve the statistical distributions of properties unique to each facies. Preliminary assessment of permeability fields derived from the

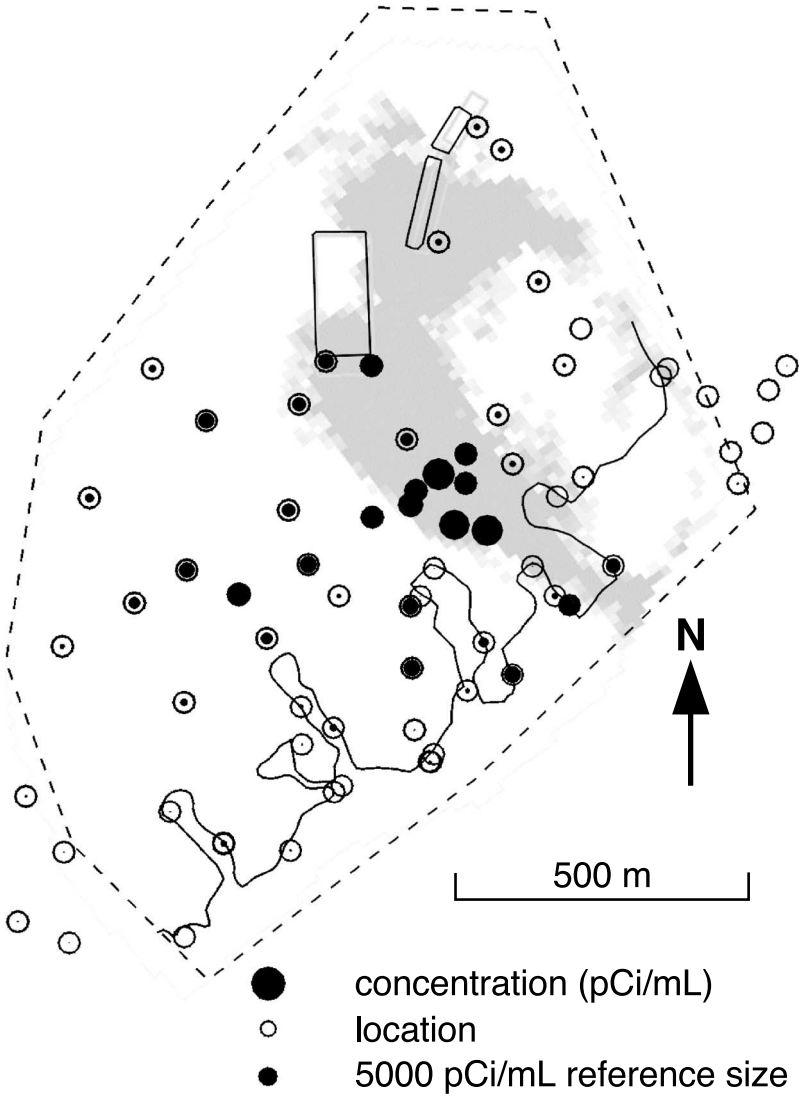

Figure 12. Tracer plume simulation using the present permeability based on high-resolution geostatistics. See Figure 2 for location of the map.

high-resolution geologic model using connectivity and streamline and tracer simulation suggests the methods were successful in identifying preferential pathways for contaminant migration from the SRS F-area seepage basins in more detail than traditional methods. Further analysis using a numerical solute transport model with rigorous boundary conditions is planned to further confirm these very promising results.

REFERENCES CITED

Colquhoun, D. J., and H. S. Johnson, Jr., 1968, Tertiary sea-level fluctuation in South Carolina: Palaeogeography, Palaeoclimatology, Palaeoecology, v. 5, p. 105–126.

Colquhoun, D. J., R. W. Oldham, J. W. Bishop, and P. D. Howell, 1982, Updip delineation of the Tertiary limestone aquifer, South Carolina: Clemson University Water-Resources Research Institute Report No. 97, 93 p.

Colquhoun, D. J., I. D. Woollen, D. S. Van Nieuwenhuise, G. G. Padgett, R. W. Oldham, D. C. Boylan, J. W. Bishop, and P. D. Howell, 1983, Surface and subsurface stratigraphy, structure and aquifers of the South Carolina coastal plain: South Carolina Department of Health and Environmental Control Report ISBN 0-9613154-0-7, 78 p.

Dennehy, K. F., D. C. Prowell, and P. B. McMahon, 1989, Reconnaissance hydrogeologic investigation of the defense waste processing facility and vicinity, Savannah River plant, South Carolina: U. S. Geological Survey Water Resources Investigations Report 88-4221, 74 p.

Fallaw, W. C., and V. Price, 1992, Outline of the stratigraphy at the Savannah River Site, *in* W. C. Fallaw and V. Price, eds., Carolina Geological Society Field Trip Guidebook, November 13–15, 1992, Geological investigations of the central Savannah River area, South Carolina and Georgia: U.S. Department of Energy and South Carolina Geological Survey, p. CGS-92-B-11-1-33.

Fallaw, W. C., and V. Price, 1995, Stratigraphy of the Savannah River Site and vicinity: Southeastern Geology, v. 35, p. 21–58.

Flach, G. P., 2002, An evaluation of dual-media contaminant transport for SRS environmental applications: Westinghouse

Savannah River Company Technical Report WSRC-TR-2002-00291 rev. 1, 242 p.

Galli A., H. Beucher, G. Le Loc'h, and B. Doligez, 1994, The pros and cons of the truncated Gaussian method, *in* M. Armstrong and P. A. Dowd, eds., Geostatistical simulations: Dordrecht, Kluwer, p. 217–233.

Harris, W. B., V. A. Zullo, R. A. Laws, and M. K. Harris, 1990, Paleogene sequence stratigraphy and chronostratigraphy of a core from Allendale County, South Carolina (abs): Geological Society of America Abstracts with Programs, v. 22, p. 17–18.

Harris, W. B., V. A. Zullo, and R. A. Laws, 1993, Sequence stratigraphy of the onshore Paleogene, southeastern Atlantic coastal plain, U.S.A.: Sequence stratigraphy and facies associations: International Association of Sedimentologists Special Publication 18, p. 537–561.

Hohn, M. E., 1988, Geostatistics and petroleum geology: New York, Van Nostrand Rienhold, 264 p.

Huddlestun, P. F., 1988, A revision of the lithostratigraphic units of the coastal plain of Georgia, the Miocene through Holocene: Georgia Geologic Survey Bulletin, v. 104, 162 p.

Huddlestun, P. F, and J. H. Hetrick, 1979, The stratigraphy of the Barnwell Group in Georgia: Georgia Geologic Survey Open-File Report 80-1, p. 56–73.

Isaaks, E. H., and R. M. Srivastava, 1989, An introduction to applied geostatistics: Oxford, Oxford University Press, 561 p.

Krige, D. G., 1951, A statistical approach to some basic valuation problems on the Witwatersrand: Journal of the Chemical, Metallurgical and Mining Society of South Africa, v. 52, p. 119–139.

Krige, D. G., 1966, Two-dimensional weighted average trend surfaces for ore valuation, *in* Proceedings of the Symposium on Mathematical Statistics and Computer Applications in Ore Valuation: South African Institute of Mining and Metallurgy, p. 13–38.

Logan, W. R., and G. M. Euler, 1989, Geology and groundwater resources of Allendale, Bamberg, and Barnwell Counties and part of Aiken County, South Carolina: South Carolina Water Resources Commission Report 155, 113 p.

Lunne, T., P. K. Robertson, and J. J. M. Powell, 1997, Cone penetration testing in geotechnical practice: New York, Routledge, 312 p.

Matheron, G. F., 1963, Principles of geostatistics: Economic Geology, v. 58, p. 1246–1266.

Matheron, G. F., 1970, La théorie des variables régionalisées et ses applications, Technical Report Fascicule 5, Les Cahiers du Centre de Morphologie Mathématique de Fontainebleau, Ecole Supérieure des Mines de Paris, 211 p.

Matheron, G. F., 1978, Estimer et choisir: Essai sur la pratique des probabilites, Fascicule 7, Les Cahiers du Centre de Morphologie Mathématique de Fontainebleau, Ecole Supérieure des Mines de Paris, 175 p.

Nystrom, P. G. Jr., and R. H. Willoughby, 1982, Cretaceous, Tertiary, and Pleistocene(?) stratigraphy of Hollow Creek and Graniteville quadrangles, Aiken County, South Carolina, *in* Geological investigations related to the stratigraphy in the Kaolin Mining District, Aiken County, South Carolina: Carolina Geological Society 1982 Field Trip Guidebook, South Carolina Geological Survey, p. 80–113.

Nystrom, P. G. Jr., R. H. Willoughby, and L. K. Price, 1989, The Cretaceous and Tertiary stratigraphy of the upper coastal plain of South Carolina, *in* Upper Cretaceous and Cenozoic geology of the southeastern Atlantic coastal plain: American Geophysical Union 28th International Geological Congress Field Trip Guidebook T171, p. 23–42.

Nystrom, P. G. Jr., R. H. Willoughby, and L. K. Price, 1991, The Cretaceous and Tertiary stratigraphy of the South Carolina upper coastal plain, *in* J. W. Horton, Jr. and V. A. Zullo, eds., Geology of the Carolinas: Knoxville, University of Tennessee Press, p. 221–240.

Pooser, W. K., 1965, Biostratigraphy of Cenozoic ostracoda from South Carolina: Arthropoda, v. 8, p. 80.

Robertson, C. G., 1990, A textural, petrographic, and hydrogeological study of the Congaree Formation at the Savannah River Site, South Carolina: Master's thesis, University of North Carolina at Wilmington, Wilmington, North Carolina, 65 p.

Robertson, C. G., and P. A. Thayer, 1992, Petrology and reservoir characteristics of the Congaree Formation at the Savannah River Site, South Carolina, in Savannah River region: Transition between the Gulf and Atlantic coastal plains, *in* Proceedings of the Second Bald Head Island Conference on Coastal Plains Geology, University of North Carolina at Wilmington, p. 54–55.

Siple, G. E., 1967, Geology and ground water of the Savannah River plant and vicinity, South Carolina: U.S. Geological Survey Water Supply Paper 1841, 113 p.

Yarus, J. M., and R. L. Chambers, 1994, Stochastic modeling and geostatistics, principles, methods, and case studies: AAPG Computer Applications in Geology, no. 3, p. 371.

Yarus, J. M., K. Yang, and K. Kramer, 2002, Practical workflows for reservoir modelling, *in* M. Armstrong, C. Bettini, N. Champigny, A. Galli, and A. Remacre, eds., Geostatistics Rio 2000: Dordrecht, Kluwer Academic Publishers, Quantitative Geology & Geostatistics Series, v. 12, p. 1–16.